

DRAFT VERSION JUNE 4, 2005

Preprint typeset using L<sup>A</sup>T<sub>E</sub>X style emulateapj v. 14/09/00RETRO-MACHOS:  $\pi$  IN THE SKY?

DANIEL E. HOLZ

Institute for Theoretical Physics, University of California, Santa Barbara, CA 93106

AND

JOHN A. WHEELER

Department of Physics, Princeton University, Princeton, NJ 08544

*Draft version June 4, 2005*

## ABSTRACT

Shine a flashlight on a black hole, and one is greeted with the return of a series of concentric rings of light. For a point source of light, and for perfect alignment of the lens, source, and observer, the rings are of infinite brightness (in the limit of geometric optics). In this manner, distant black holes can be revealed through their reflection of light from the Sun. Such retro-MACHO events involve photons leaving the Sun, making a  $\pi$  rotation about the black hole, and then returning to be detected at the Earth. Our calculations show that, although the light return is quite small, it may nonetheless be detectable for stellar-mass black holes at the edge of our solar system. For example, all (unobscured) black holes of mass  $M$  or greater will be observable to a limiting magnitude  $\bar{m}$ , at a distance given by:  $0.02 \text{ pc} \times \sqrt[3]{10^{(\bar{m}-30)/2.5} (M/10 M_{\odot})^2}$ . Discovery of a Retro-MACHO offers a way to *directly* image the presence of a black hole, and would be a stunning confirmation of strong-field general relativity.

*Subject headings:* gravitational lensing—black hole physics—relativity

## 1. INTRODUCTION

In the discovery of MACHOs light has shown its power to reveal dark compact objects. In these events the photon from a distant source suffers a very small angular deflection, small enough to make gravitational lensing the relevant mechanism. The bending power of a black hole is not limited, however, to small angles but reaches to  $\pi$  and odd multiples of  $\pi$ . Illuminated by a powerful point source of light, the black hole therefore will shine back with a series of concentric rings (we call this retrolensing). A waterdrop, too, likewise illuminated, shines back, but for a different reason: the internal reflections experienced by the photons. That returned light shows to the air traveler flying over a fogbank as a “glory”: a rainbow-like halo surrounding the shadow of the plane on the cloud. Each ray of light that contributes to this sensation has suffered its  $\pi$  deflection in a different waterdrop, therefore the impression of colored rings that the glory makes is impression only, built up in the last analysis out of multitudes of tiny dots of illumination. No one would be so rash as to expect a detectable backscatter from a single water droplet. It is precisely the search for such backscatter from a single black hole (the putative retro-MACHO) that is, however, the topic of this paper.

How search for retro-MACHOs, for “ $\pi$  in the sky”, especially when dogged by the negative implications of the familiar phrase? To tell observers to go and look everywhere is to them as dismaying as to be told to look nowhere. Fortunately the successful search for MACHOs provides a helpful model, and the records from that search an immediate place of reference. Recent microlensing events appear to directly confirm that a population of stellar-mass black holes exists in our galaxy (Bennett et al. 2001; Mao et al. 2002; Agol et al. 2002). The Sun, in turn, furnishes a powerful nearby source with whose help one can hope

to search a nearby region of the galaxy for black holes not otherwise revealed, taking advantage of times when the Earth interposes itself to spare the registering device from the direct glare of the light source. Although the observation of a retro-MACHO is unlikely, it nonetheless affords one of the few ways to directly image nearby black holes, and if ever observed, would make for an impressive confirmation of Einstein’s theory.

## 2. WHAT IS A RETRO-MACHO?

Consider a point source of light, an observer, and a black hole lens, with all three co-linear and the observer located *in between* the source and black hole. The observer, looking at the image of the source in the black hole, will see (resulting from symmetry) an (infinite) series of concentric rings, corresponding to bending angles of successively higher odd multiples of  $\pi$ . The outermost ring would be from photons suffering a  $\pi$  deflection, the next inner ring corresponding to a  $3\pi$  deflection, and so on. For a point source, and in the limit of geometric optics, the amplification of the rings is infinite. For realistic scenarios with extended sources, however, the amplification is finite. For example, consider an extended spherically symmetric source emitting uniformly across its surface. The image of the source at the observer is an annulus, where the outer and inner radii correspond to the appropriate impact parameters for photons coming from the top and bottom parts of the source, as shown in Fig. 1. Since lensing conserves surface brightness, the brightness of the ring image relative to that of the source is given by the ratio of the areas of the images, as seen at the observer.

The fraction of the sky covered by the ring image is given by:

$$A_I = \frac{\pi b_o^2 - \pi b_i^2}{4\pi D_{OL}^2}, \quad (1)$$

where  $b_i$  and  $b_o$  are the impact parameters corresponding to the inner and outer radii of the ring, respectively. Note that the impact parameter is not the same as the periastron (closest approach) distance:

$$b = \frac{r}{\sqrt{1 - 2M/r}}, \quad (2)$$

where  $b$  is the impact parameter,  $r$  is the periastron distance, and  $M$  is the mass of the black hole. Throughout we measure all quantities in geometric units, with  $G = c = 1$  (e.g.,  $1 M_\odot = 1.5 \text{ km}$ ).

This is to be compared with the sky coverage of the source, as seen directly by the observer:

$$A_S = \frac{\pi R_S^2}{4\pi D_{OS}^2}. \quad (3)$$

The total amplification,  $\mu$ , of the image is given by the ratio of their sky coverages, yielding

$$\mu = \frac{b_o^2 - b_i^2}{R_S^2} \left( \frac{D_{OS}}{D_{OL}} \right)^2. \quad (4)$$

To calculate the brightness of the image we need to know the inner and outer radii of the ring, represented by rays from points  $A$  and  $B$  in Fig. 1, respectively. Rays from  $A$  suffer a deflection angle of  $\pi - \alpha$ , while for those from  $B$  the deflection is  $\pi + \alpha$ , where  $\alpha = R_S/D_{LS}$ . In everything that follows, we restrict our attention to the primary (outermost, brightest) images, although a whole succession of images is present (corresponding to higher odd multiples of  $\pi$ ). For the sake of simplicity, we confine ourselves to the case of non-rotating (Schwarzschild) black holes. The calculations for rotating (Kerr) holes are significantly more complex (Rauch & Blandford 1994), and will be deferred to later work. To calculate the impact parameters that correspond to the necessary deflection angles, we take advantage of an approximate expression in Luminet (1979) (see also Chandrasekhar (1983)) for the case of large deflection:

$$b = b_c + b_d e^{-\Theta}, \quad (5)$$

where  $b_c = 3\sqrt{3}M$ ,  $b_d = 648\sqrt{3}e^{-\pi}M(\sqrt{3}-1)^2/(\sqrt{3}+1)^2 \approx 3.4823M$ , and  $\Theta$  is the deflection angle. Chandrasekhar also provides exact analytic forms for the solution (in terms of Elliptic functions). We find that the approximate expressions are within 10% of the exact values for bend angles satisfying  $\Theta \geq \pi/4$ , and are good to within 1/2% for bend angles with  $\Theta \geq \pi$ .

Using the results of eq. 5 to calculate  $b_o$  and  $b_i$ , eq. 4 can be simplified to

$$\mu \simeq 3.22 M^2 \frac{D_{OS}^2}{R_S D_{LS} D_{OL}^2}. \quad (6)$$

Eq. 6 assumes perfect (colinear) alignment of the source, observer, and lens. The generic case, of course, will involve misalignment, as shown in Fig. 2. We define the misalignment angle,  $\beta$ , to be the angle between the source-observer line and the observer-lens line, as measured at the observer (such that  $\beta = 0$  corresponds to the case of perfect alignment shown in Fig. 1). As  $\beta$  increases from zero the ring

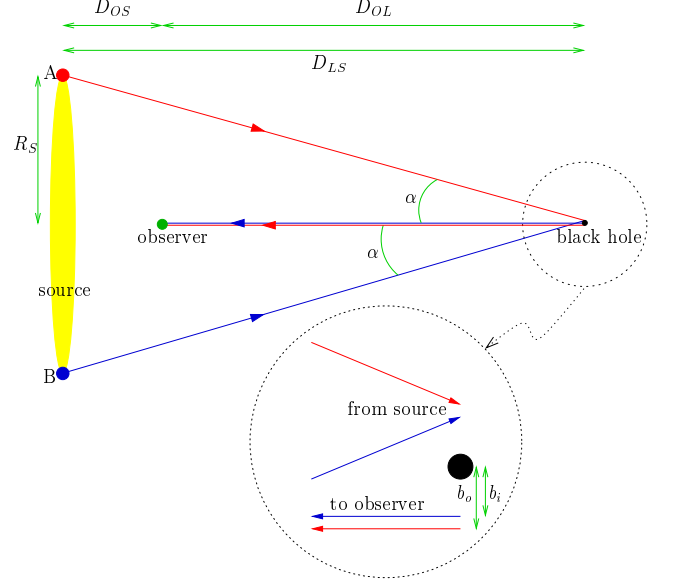


FIG. 1.— Perfect alignment: the (extended) source, observer, and lens are colinear. The resulting image of the source, as lensed by the black hole, is a ring. (The angles in this figure are greatly exaggerated.)

splits into two arcs (on either side of the lens), centered on the lens-observer-source plane (see the inset of Fig. 2), with the arcs shrinking to small, point-like images as  $\beta$  approaches  $\pi/2$ . The tangential extent of these arcs, as seen at the observer, is determined by the angular extent of the protrusion of the source out of the plane of Fig. 2:  $\Delta\Theta \approx 2 \tan^{-1}(R_S/D_{OS} \sin \beta)$ . The total area of each image is thus found to be

$$A_{\text{image}} = \pi(b_o^2 - b_i^2) \times \frac{\Delta\Theta}{2\pi} \quad (7)$$

$$= (b_o^2 - b_i^2) \tan^{-1} \left( \frac{R_S}{D_{OS} \sin \beta} \right), \quad (8)$$

where we have neglected the fact that the image heights taper down to zero at their edges. Here  $b_o$  and  $b_i$  represent the outer and inner apparent impact parameters of the images, which correspond to bend angles of  $(\pi - \delta) \mp \alpha$  for the bigger image, and  $(\pi + \delta) \mp \alpha$  for the smaller image. Note that, since surface brightness is conserved, the bigger image is also the brighter one (and is found further from the center of the lens, on the side opposite that of the source). The magnification of each image is again given by the ratio of the areas of the source and image, namely:

$$\mu = (b_o^2 - b_i^2) \tan^{-1} \left( \frac{R_S}{D_{OS} \sin \beta} \right) \frac{D_{OS}^2}{\pi R_S^2 D_{OL}^2}. \quad (9)$$

In the limit  $\beta \rightarrow 0$ , and summing up both images, eq. 9 goes over to eq. 4, as expected. Using eq. 5, and taking both  $\alpha \ll 1$  and  $\beta \ll 1$ , the combined magnification of both images simplifies to

$$\mu \simeq 3.22 M^2 \frac{D_{OS}^2}{R_S D_{LS} D_{OL}^2} - 2.05 \beta M^2 \frac{D_{OS}^3}{R_S^2 D_{LS} D_{OL}^2}. \quad (10)$$

### 3. SOURCES FOR RETRO-MACHOS

Every source of light on the sky has the potential to be lensed by a retro-MACHO (in the same manner that

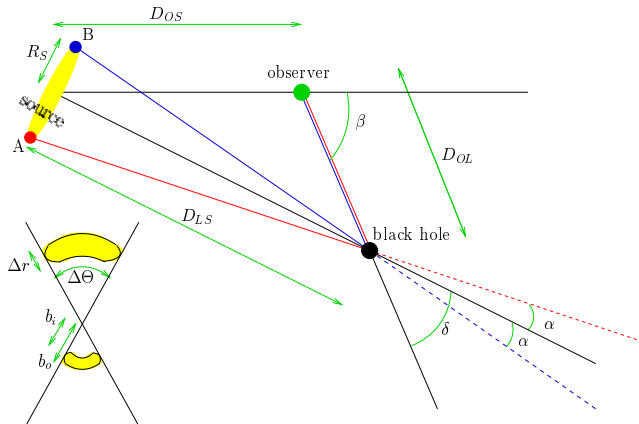


FIG. 2.— Imperfect alignment: the source, observer, and lens are not colinear. Pairs of images are produced, centered on the source–observer–lens plane, on opposite sides of the lens (see inset).

the entire Universe is imaged near the horizon of each and every (unobscured) black hole). However, given the very slight magnification, only the very brightest of sources, with the most felicitous of alignments, will be observable.

We envisage the retro-MACHO to sit at one or another distance and ask for its expected luminosity in order to compare it with familiar objects in the sky. In each case we take the primary source of illumination to be the Sun (output  $I = 4 \times 10^{33}$  erg/sec, apparent visual magnitude  $m = -26.8^m$ ). In Table 1, we show the observed apparent visual magnitudes of these hypothetical solar retro-MACHOs. In addition to perfect alignment ( $\beta = 0$ ), it is also useful to consider the case of edge alignment ( $\beta = R_S/D_{OS} = R_{\odot}/1 \text{ AU}$ ), wherein the observer–lens line grazes the edge of the source. Because of its large angular size (as seen from Earth), the Sun offers the best opportunities for close alignment. In Eq. 9 we find that the Sun’s  $1/2^\circ$  angular size dominates over smaller values of  $\beta$  for other sources.

A number of other potential sources, in addition to the Sun, are worth mentioning. Consider Sirius, the next brightest star in the sky. For a perfectly-aligned retro-MACHO of  $1 M_{\odot}$ , at a distance of 0.01 pc, the retro-image of Sirius would appear at  $34^m$ . A misalignment of  $1^\circ$  would put its brightness at  $51^m$ . The red giant Betelgeuse would have a brightness of  $39^m$  perfectly aligned, and drop to  $53^m$  when  $\beta = 1^\circ$ . These are to be compared to the Sun, which has a retro-image at  $31^m$  for perfect alignment. For  $\beta = 1^\circ$  this drops by only 3 mag, to  $34^m$ , showing the advantage of the Sun’s large angular size.

As the magnification factors in eqs. 6 and 10 scale as  $M^2$ , one might be tempted to consider the supermassive black hole at the galactic center as a retro-MACHO lens. The Sun, at its closest ( $5^\circ$ ) alignment with the galactic center black hole, has a retro-image brightness of  $50^m$ . This becomes even fainter when the considerable extinction to the galactic center (double the usual value, as the photons travel round trip) is taken into account.

It is to be noted that all of the expressions found in this paper become relevant for black holes at cosmological distances by replacing the physical distances with the appropriate cosmological luminosity distances. One can imagine imaging the Milky Way galaxy in the supermassive black hole of a nearby galaxy.

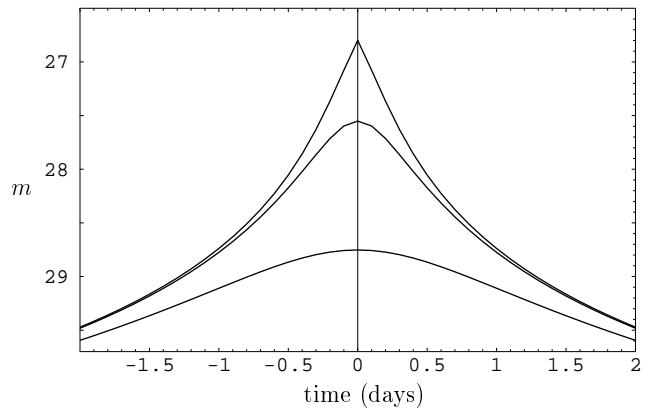


FIG. 3.— Solar retro-MACHO lightcurves: The apparent visual magnitude,  $m$ , of the Sun, imaged in a  $10 M_{\odot}$  black hole at a distance of 0.01 pc. The different curves are for the black hole at angular displacements from the ecliptic plane of  $0$ ,  $R_{\odot}/1 \text{ AU}$ , and  $1^\circ$  respectively (top to bottom).

However, even if Andromeda had an unobscured central supermassive black hole, the image of the Milky Way would be dimmer than  $70^m$ . In more extreme cases, we could imagine a supernovae or quasar imaged (in any frequency band, e.g. radio) in a distant supermassive black hole. Even for perfect alignments, such scenarios produce extremely dim images.

#### 4. PROPERTIES OF RETRO-MACHOS

A retro-MACHO would appear somewhat like a conventional MACHO. However, rather than magnifying a pre-existing star, a retro-MACHO causes a “star” to appear out of nowhere. A number of sample retro-MACHO lightcurves are shown in Fig. 3. The colors of a retro-MACHO are identical to those of the source, and this will provide an important way to confirm the nature of such events. The structure of a retro-MACHO will be unresolvable (much like the multiple images in microlensing are unresolvable), as the radius of the ring is on the order of the Schwarzschild radius of the lens. Even for very close black holes (say, at the edge of the solar system), the angular extent of a retro-MACHO image remains less than a milliarcsec.

As in the MACHO case, the timescale of retro-MACHO events is determined by the relative motion of the source, lens, and observer. However, rather than the Einstein angle of the lens being the relevant angular scale, in the retrolensing case we are interested in the angular extent of the source measured at the observer. We define the timescale of an event to be given by the length of time it takes to go from perfect alignment to edge alignment:

$$t = \frac{D_{OL}}{v} \frac{R_S}{D_{LS}}, \quad (11)$$

where  $v$  is the transverse velocity of the observer with respect to the source–lens line-of-sight. The Sun’s angular extent is  $1/2^\circ$ , which means that a solar retro-MACHO lasts about  $1/2$  day, assuming the source–lens motion is stationary as compared to the motion of the Earth about the Sun. For lens motion at galactic velocities ( $\sim 200 \text{ km/sec}$ ), the timescale for the lens to move an appreciable angle on the sky is considerably longer (unless the lens is within the solar system). For the case of distant stars being retro-lensed by distant black holes, however, the timescales can shorten because of the extremely

small angles needed for edge alignment. The retro-image of Sirius in a black hole about a parsec away can be expected to last on the order of hours, with the precise value depending on the relative projected velocities.

Another point of consideration is the light travel-time of a given retro-MACHO event. For example, for a solar retro-MACHO at a distance of a parsec, the event will appear on the sky corresponding to a position directly opposite to where the Sun was located  $2\text{ pc}/c \approx 6$  years ago! For a retro-MACHO to occur within  $1^\circ$  of the current antipodal position of the Sun, the black hole must be within about a day's round-trip light travel time, putting the black hole lens at the distance of Pluto.

In addition, solar retro-MACHO events will repeat annually, as the Earth returns to the appropriate alignment spot in the ecliptic. This annual repetition may become one of the most valuable signatures of retro-MACHOs, and can be used both to identify candidates in sky surveys, and to confirm the nature of the events.

## 5. OBSERVING STRATEGIES

From Table 1, it is apparent that retro-MACHOs are exceedingly dim, even in the best of circumstances. The most likely observed retro-MACHO would be our Sun imaged in a nearby stellar-mass black hole. Simple theoretical estimates give a value for the local number density of stellar-mass black holes of  $N_{\text{BH}} \sim 8 \times 10^{-4}/\text{pc}^3$  (Shapiro & Teukolsky 1983). Based on the microlensing event rates towards the galactic bulge of the MACHO and OGLE teams, we find  $N_{\text{BH}} \sim 2 \times 10^{-4}/\text{pc}^3$  (Agol & Kamionkowski 2001; Alcock et al. 2001). Both these rates include black holes in the mass range  $5 M_\odot \lesssim M_{\text{BH}} \lesssim 15 M_\odot$ . Although it is unlikely for there to be a stellar-mass black hole within a parsec, it is reasonable to expect one within 10 pc of the Sun. Such a black hole, if perfectly aligned with the Sun (i.e. in the ecliptic plane), would produce a  $49^m$  retro-image of the Sun. Even at a distance of 1 pc, the image only brightens to  $41^m$ . The earliest population of stars are thought to have masses in the  $300\text{--}1,000 M_\odot$  range, and probably collapse to form black holes in a similar mass range (see, e.g., Fryer, Holz, & Hughes (2001)). The retro-MACHOs from these holes would be visible at  $32^m$  to a distance of over a parsec. It is apparent, however, that even in the best of circumstances only a chance encounter with an unusually nearby or massive black hole will lead to an observable retro-MACHO.

Microlensing surveys have produced a number of candidate black hole lenses. These arise from long-timescale events, where the parallax effect of the Earth's revolution about the Sun is strong enough to break some of the degeneracies in the microlensing fits. For example, the best fit to MACHO galactic bulge event 96-BLG-5 is a black hole of mass  $6 M_\odot$  at a distance of 1 kpc (Bennett et al. 2001; see also Agol et al. 2002). Although this is too distant to be observed, it is conceivable that a future microlensing event may provide us with a definite retrolensing candidate. In these cases we know exactly where and when to look, and what to expect.

Although the likelihood is small, a close approach of a stellar-mass black hole would have a potentially cata-

trophic impact on our solar system (both through disruption of the Oort cloud, and through direct effects on the orbital stability of the planets). Retrolensing offers perhaps the only *direct* observational signature of such an incoming “rogue” black hole. The Sun can be considered a searchlight, sweeping out a  $1/2^\circ$ -wide swath of the sky centered on the ecliptic plane in search for black holes. For a magnitude limit of  $\bar{m}$ , this reveals all black holes of mass  $M$  or greater out to a limiting distance of  $0.02\text{ pc} \times \sqrt[3]{10^{(\bar{m}-30)/2.5} (M/10 M_\odot)^2}$ . Through repeated, deep observations of the direction anti-podal to the Sun, retrolensing can be utilized to construct a black hole early warning system.<sup>1</sup> Consider Nemesis, a hypothetical solar companion (Hills 1985). If we take Nemesis to be a  $1 M_\odot$  black hole at the outer edge of the Oort cloud ( $D_{\text{OL}} = 9 \times 10^4\text{ AU}$ ), and lying near the ecliptic, it would be directly imaged as a retro-MACHO at  $43^m$ . However, such a Nemesis *would* be revealed ( $m < 30^m$ ) if it approached to a distance of  $D_{\text{OL}} \lesssim 10^3\text{ AU}$ . It is to be noted that microlensing, although quite proficient at detecting compact objects in the direction of the galactic bulge at distances of kiloparsecs, is not particularly efficient at detecting nearby black holes. The Einstein angle of a point mass lens is given by  $\theta_E = \sqrt{4MD_{\text{LS}}/(D_{\text{OL}}D_{\text{OS}})}$ , which for distant stars lensed by nearby masses simplifies to  $\theta_E \approx \sqrt{4M/D_{\text{OL}}}$ . For a black hole at  $D_{\text{OL}} = 10^3\text{ AU}$ , a star would have to be aligned to within  $1.5\text{ arcsec}$  to be microlensed. For a solar retro-MACHO, on the other hand, edge-alignment is automatically satisfied for any black hole lying within  $1/4^\circ$  of the ecliptic. Retrolensing is thus better than microlensing for detecting approaching nearby black holes.

We are entering an age where the entire sky can be expected to be imaged deeply, and all transient objects noted (Blandford 2001). Within any such large, repetitive sample, a retro-MACHO would look like a MACHO event with zero baseline flux (i.e. no background star). Upon detecting such an event, one would try to identify a possible light source at the diametrically opposite position on the sky (“through” the Earth). Does the source have identical colors to the transient image? If so, retro-MACHO! For example, in the case of the Sun, we would look for images with precisely solar spectra. It may be of interest to perform a thorough search of extant microlensing survey databases for events that do not correspond to amplification of background stars. Presuming a non-detection of such events, and taking the depth of current surveys to be  $\sim 22^m$ , we can directly rule out unobscured black holes with mass greater than  $10 M_\odot$  in the direction of the galactic bulge ( $\beta \geq 5^\circ$ ) at distances less than 150 AU. These distance limits improve dramatically with deeper surveys.

Should a retro-MACHO ever be observed, it would afford an unprecedented opportunity to study the strong-field aspects of general relativity. These objects probe very near the horizon of the holes—in the perfect alignment case, the image represents photons that have passed within  $3.5m = 1.75r_s$  of the singularity (where  $r_s$  is the Schwarzschild radius), as deep into the strong field regime

<sup>1</sup> It is to be noted that a very powerful ( $>$  Gigawatt) laser can be used to *actively* probe for retro-MACHOs. One could scan the entire sky systematically, and monitor for returning glints of light (in the same frequency band as that of the laser, and with time delays a direct measure of distance to the black holes). This would constitute a true black hole early warning system.

as we are ever likely to probe via light. A retro-MACHO observation would be an impressive confirmation of the theory of general relativity, and would leave little doubt as to the existence of Einstein black holes.

It is a pleasure to acknowledge discussions with Eric

Agol, Doug Eardley, Warner Miller, Bohdan Paczyński, James Peebles, Sterl Phinney, Bob Rutledge, and John-dale Solem in the course of this work. We thank Emily Bennett for providing invaluable assistance in the preparation of the manuscript.

## REFERENCES

- Agol, E. & Kamionkowski, M. 2002, MNRAS, 334, 553  
 Agol, E., Kamionkowski, M., Koopmans, L.V.E., & Blandford, R.D. 2002, [astro-ph/0203257](#)  
 Alcock, C. et al. 2001, ApJ, 550, L169  
 Bennett, D.P. et al. 2001, [astro-ph/0109467](#)  
 Blandford, R.D. 2001, PASP, 113, 1309  
 Chandrasekhar, S. 1983, *The Mathematical Theory of Black Holes* (Oxford: Oxford University Press)  
 Fryer, C.L., Holz, D.E., & Hughes, S.A. 2002, ApJ, 565, 430  
 Hills, J.G. 1985, AJ, 90, 1876  
 Luminet, J.-P. 1979, A&A, 75, 228  
 Mao, S. et al. 2002, MNRAS, 329, 349  
 Rauch, K.P. & Blandford, R.D. 1994, ApJ, 421, 46  
 Shapiro, S.L. & Teukolsky, S.A. 1983, *Black Holes, White Dwarfs, and Neutron Stars* (New York: Wiley)

TABLE 1  
RETRO-MACHO BRIGHTNESSES OF THE SUN

BH mass ( $M_{\odot}$ )	BH distance (pc)	$\beta = 0$ (perfect alignment)	$\beta = R_{\odot}/1 \text{ AU}$ (edge alignment)	$\beta = 1^{\circ}$	$\beta = \pi/4$	$\beta = \pi/2$ (max misalignment)
1	$10^{-2}$	31.0	32.6	34	38	38
1	$10^{-1}$	38.6	40.1	41	45	46
10	$10^{-2}$	26.1	27.6	29	33	33
10	$10^{-1}$	33.6	35.1	36	40	41
10	1	41.1	42.6	44	48	48